Eastern Washington University
EWU Digital Commons

Chemistry and Biochemistry Faculty Publications   Chemistry and Biochemistry

12-31-2007

Muon-Fluorine Entangled States In Molecular Magnets

T Lancaster

S J. Blundell

P J. Baker

M L. Brooks

W Hayes

See next page for additional authors

Follow this and additional works at: http://dc.ewu.edu/chem_fac

Part of the Chemistry Commons

Recommended Citation

Authors

T Lancaster, S J. Blundell, P J. Baker, M L. Brooks, W Hayes, F L. Pratt, Jamie L. Manson, M M. Conner, and J A. Schlueter

Muon-fluorine entangled states in molecular magnets

T. Lancaster,[1, *] S.J. Blundell,[1] P.J. Baker,[1] M.L. Brooks,[1] W. Hayes,[1]
F.L. Pratt,[2] J.L. Manson,[3] M.M. Conner,[3] and J.A. Schlueter[4]

[1]*Clarendon Laboratory, Oxford University Department of Physics, Parks Road, Oxford, OX1 3PU, UK*
[2]*ISIS Facility, Rutherford Appleton Laboratory, Chilton, Oxfordshire OX11 0QX, UK*
[3]*Department of Chemistry and Biochemistry, Eastern Washington University, Cheney, WA 99004, USA*
[4]*Material Science Division, Argonne National Laboratory, Argonne, IL 60439, USA*

The information accessible from a muon-spin relaxation experiment is often limited since we lack knowledge of the precise muon stopping site. We demonstrate here the possibility of localizing a spin polarized muon in a known stopping state in a molecular material containing fluorine. The muon-spin precession that results from the entangled nature of the muon-spin and surrounding nuclear spins is sensitive to the nature of the stopping site and we use this property to identify three classes of site. We are also able to describe the extent to which the muon distorts its surroundings.

PACS numbers: 76.75.+i, 75.50.Xx, 61.18.Fs

Muon-spin relaxation (μ^+SR) continues to provide insights into the nature of magnetic materials, superconductors, semiconductors, soft matter and chemical reactions [1]. The technique involves stopping spin polarized muons in a target sample where the muons probe the distribution of local magnetic fields across the muon stopping sites. Despite its successes, two concerns are sometimes raised. The first is that the exact muon stopping site in a material is, in general, not precisely known, introducing some uncertainty in the determination of the local spin structure. This is especially applicable in anisotropic or chemically complex materials where a number of different candidate stopping sites exist. A second objection is that it is not possible to quantify the degree to which the presence of the charged muon distorts its surroundings and hence to estimate the modification of superexchange pathways that could, in principle, affect the local spin structure. Here we show that in addition to the magnetic behavior usually probed by μ^+SR, the entangled states of μ^+ spin and ^{19}F nuclear spins allow the accurate determination of the muon site in a class of novel fluorinated molecular magnets, along with an estimate of the distortion introduced by the presence of the probe particle.

Localized muons in solids often interact with their environment via dipole-dipole coupling. In many cases the large number of spin centres surrounding the muon allow the use of the local magnetic field (LMF) approximation, where the muon spin S interacts with the net local magnetic field at the muon site $\langle B \rangle$ via the Hamiltonian $\mathcal{H} = \gamma_\mu S \cdot \langle B \rangle$, where γ_μ is the muon gyromagnetic ratio. For the commonly encountered case of the muon response to an ensemble of randomized static local fields, the LMF model gives the Kubo-Toyabe function [2], which is well approximated by a Gaussian function $\exp(-\sigma^2 t^2)$ at early times. Occasionally, however, the muon is found to interact strongly with a small number of spin centres through dipole coupling [3, 4], a process

which is described by the Hamiltonian

$$\mathcal{H} = \sum_{i>j} \frac{\mu_0 \gamma_i \gamma_j}{4\pi r^3} \left[\mathbf{S}_i \cdot \mathbf{S}_j - 3(\mathbf{S}_i \cdot \hat{\mathbf{r}})(\mathbf{S}_j \cdot \hat{\mathbf{r}}) \right], \qquad (1)$$

where $\mathbf{r}$ is the vector linking spins S_i and S_j, which have gyromagnetic ratios $\gamma_{i,j}$. This strong interaction is found most often in materials containing fluorine, for two reasons: fluorine is the most electronegative element, causing muons to localise in its vicinity and fluorine occurs with a single isotope (^{19}F) with an $I = 1/2$ nuclear spin, giving rise to a strong μ^+SR signal as a result of the interaction (see below). For example, in most insulating metal fluorides [5] the muon sits midway between two fluorine ions forming a strong linear "hydrogen bond" with an F–F separation of $d = 0.238$ nm, which is approximately twice the fluorine ionic radius. This stopping state (the so-called F–μ^+–F) is similar to the V_k centre observed in alkali halides, which is often treated as a molecule-in-a-crystal defect [6], where the host weakly perturbs the molecular ion.

The fact that the spins are not initially in an eigenstate of the Hamiltonian in Eq. (1) causes a time dependence of the system's total wavefunction, visualised classically as spontaneous precession of all spin species. The observed property in μ^+SR is the polarization $D_z(t)$ of the muon ensemble along a quantization axis z, which is given by [7]

$$D_z(t) = \frac{1}{N} \left[\sum_{m,n} |\langle m|\sigma_z|n\rangle|^2 \cos(\omega_{mn} t) \right], \qquad (2)$$

where N is the number of spins, $|m\rangle$ and $|n\rangle$ are eigenstates of the total Hamiltonian $\mathcal{H}$ and σ_z is the Pauli spin matrix corresponding to the quantization direction.

These considerations suggest that, in compounds containing fluorine ions, muons might be localized in known positions near fluorines. The muon and fluorine spins then become entangled causing the spins to evolve via
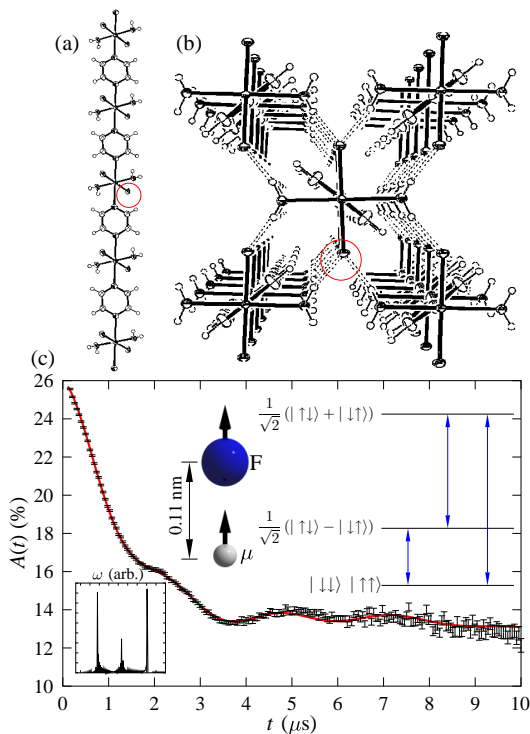
FIG. 1: (Color online) (a) Linear chain structure of $CuF_2(H_2O)_2(pyz)$. The circled regions shows sample fluorine atoms near which the muon is expected to localize. (b) Crystal packing viewed parallel to the chain axis. Dotted lines show F H–O hydrogen bonds. (c) Example ZF μ^+SR spectrum measured at $T = 3.4$ K with a fit to the F–μ^+ dipole interaction described in the text. *Inset:* F–μ^+ configuration, (top right) the resulting energy levels with allowed transitions and (bottom left) the calculated frequency spectrum.

the Hamiltonian in Eq.(1) and the sensitivity of the interaction to the relative positions of the spin centres allows the spin configuration and stopping site to be determined. This is indeed the case in a novel class of fluorine-containing molecular magnets. The stopping states, however, are more complex than the linear F–μ^+-F molecular ion previously observed in many inorganic insulating fluorides [5].

Molecular magnets are self assembled materials which are formed through bridging paramagnetic cation centres (such as Cu^{2+} in the compounds studied here (see Table I)) with organic ligands. These materials often possess low-dimensional (i.e. 2D, 1D) structural motifs and correspondingly display low-dimensional magnetic properties [8]. Our recent experiments on such systems have shown that muons are uniquely sensitive to the presence of long-range magnetic order [9]. Below the antiferromagnetic transition at T_N we observe oscillations in the time dependence of the muon polarization (the "asymmetry" $A(t)$ [1]) which are characteristic of a quasi-static local magnetic field at the muon stopping site. In the

LMF model, this local field causes a coherent precession of the spins of those muons for which a component of their spin polarization lies perpendicular to this local field (expected to be 2/3 of the total spin polarization for a powder sample). The frequency of the oscillations is given by $\nu_i = \gamma_\mu |B_i|/2\pi$, where γ_μ is the muon gyromagnetic ratio ($= 2\pi \times 135.5$ MHz T^{-1}) and B_i is the average magnitude of the local magnetic field at the ith muon site. Above T_N the character of the measured spectra changes considerably and we observe lower frequency oscillations characteristic of the dipole interaction of the muon and the ^{19}F nucleus. The Cu^{2+} electronic moments, which dominate the spectra for $T < T_N$, are no longer ordered in the paramagnetic regime, and fluctuate very rapidly on the muon time scale. They are therefore motionally narrowed from the spectra, leaving the muon sensitive to the quasistatic nuclear magnetic moments. The signal arising from F–μ^+ states persist in these materials to temperatures well above 100 K.

In fluorinated materials, where the muon-spin is relaxed through interaction with nuclear moments, we expect two contributions to the μ^+SR spectra. The first is from muons that strongly couple to fluorine nuclei, which give rise to contributions derived from Eq. (2). Note that since our measurements are carried out on powder samples, $D_z(t)$ also includes the effect of angular averaging. The second contribution is from those muons weakly coupled to a large number of nuclei, leading to Gaussian relaxation in the LMF model, as described above. Above the critical temperature T_N, spectra were found to be well described by the resulting polarization function

$$A(t) = A_0[p_1 D_z(t) \exp(-\lambda t) + p_2 \exp(-\sigma^2 t^2)] + A_{bg}, \quad (3)$$

where A_0 is the signal arising from the sample, $p_1 + p_2 = 1$, and A_{bg} accounts for those muons that stop in the sample holder or cryostat tails.

Below we discuss experimental results[10] for three molecular materials where stopping states arise that are different from the conventional F–μ–F state and exemplify three distinct classes of implanted muon state.

Case I: Interaction with a single fluorine. The compound $CuF_2(H_2O)_2(pyz)$ [11] is formed from $CuF_2O_2N_2$ octahedra linked with pyrazine bridges along the a-direction to form linear chains (Fig. 1(a)). Extensive hydrogen bonding interactions tether the chains into the 3D network shown in Fig. 1(b). The material undergoes an AFM transition at $T_N = 2.54(8)$ K below which oscillations in the muon asymmetry are observed [11]. ZF μ^+SR spectra measured on $CuF_2(H_2O)_2(pyz)$ above T_N are shown in Fig. 1(b) where we see slow, heavily damped oscillations characteristic of F–μ^+ dipole coupled states. The spectra are most successfully modelled by assuming the muon is strongly coupled with a single $I = \frac{1}{2}$ F spin, localized a distance $d = 0.110(2)$ nm away from a fluorine nucleus. The resulting energy level structure and allowed transitions for this scenario are shown inset in

TABLE I: Parameters for Eq.(3) for each material studied. with resulting χ^2 for the fits described in the main text. $\chi^2_{F\mu F}$ corresponds to the best fits obtained using a conventional F–μ^+–F model for comparison.

	p_1	λ	p_2	σ	χ^2	$\chi^2_{F\mu F}$
$CuF_2(H_2O)_2(pyz)$	0.43	0.36	0.57	0.56	1.2	1.6
$CuNO_3(pyz)_2PF_6$	0.65	0.24	0.35	0.45	2.2	4.1
$[Cu(HF_2)(pyz)_2]ClO_4$	0.73	0.24	0.27	0.43	2.2	3.9

Fig. 1(c). The F–μ^+ spin system consists of three distinct energy levels with three allowed transitions between them giving rise to the distinctive three-frequency oscillations observed (inset Fig. 1c). The signal is described by a polarization function $D_z(t) = \frac{1}{6}\left[1 + \sum_{j=1}^{3} u_j \cos(\omega_j t)\right]$, where $u_1 = 2$, $u_2 = 1$ and $u_3 = 2$. The transition frequencies (shown in Fig. 1(c)) are given by $\omega_j = j\omega_d/2$ where $\omega_d = \mu_0 \gamma_\mu \gamma_F / 4\pi r^3$, and r is the F–μ^+ separation. The resulting fit is shown in Fig. 1(c) using the parameters listed in Table I.

We note first that the strong interaction of the muon and a single F is unusual. However, a muon stopping site between two fluorines is probably made energetically unfavourable due to the presence of the protons on the H_2O groups which are hydrogen bonded to the fluorines (and stabilize the solid). In this material the smallest F–F distance (between adjacent chains) is 0.34 nm and a position midway between these two fluorines invariably lies very close (~ 0.13 nm) to the protons on a H_2O group. We further exclude a muon site in $CuF_2(H_2O)_2pyz$ where the muon is bonded to F but sits near the protons on the H_2O groups since fits to such a configuration are not able to account for the measured data. It is more probable that the muon's separation from the F ion is not precisely in the a-b plane, but rather has a small component in the c direction, taking it closer to the electron density on the aromatic rings. We note further that we have also observed coupling of the muon to a single F in the polymer PVDF ($-(CH_2CF_2)_n-$) below the polymer glass transition [15]. This demonstrates that this stopping state is not unique.

Case II: Crooked F-F bond with the PF_6^- ion. The quasi 2D compound $[Cu(NO_3)(pyz)_2]PF_6$ [12, 13] is formed from infinite 2D sheets of $[Cu(pyz)_2]^{2+}$ lying in the ab plane. These are linked along the c-direction by NO_3^{2-} ions. The PF_6^- anions occupy the body-centred positions within the pores. The PF_6^- anion has a regular octahedral geometry with a P–F distance of 0.157 nm.

Our measurements show that this material magnetically orders below $T_N = 2.0(2)$ K. Above T_N we again observe a signal from dipole coupling. An example spectrum measured above T_N is shown in Fig. 2. Although one would expect the muon to localise near a PF_6 anion, it is not clear *a priori* how many fluorine centres will be strongly coupled to the muon spin. Modelling
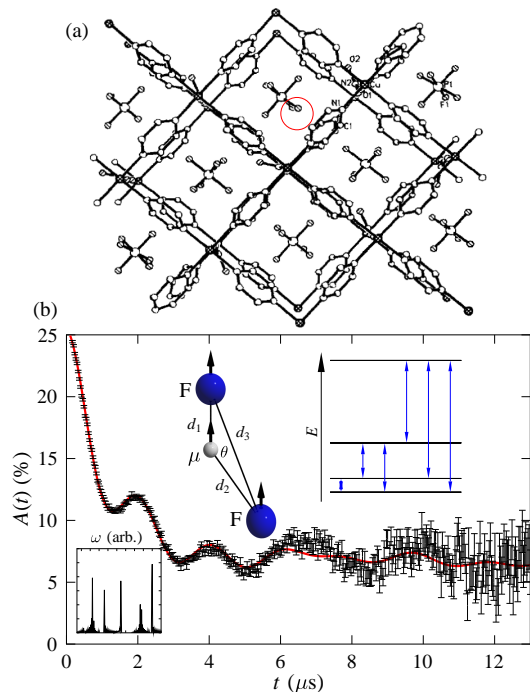

FIG. 2: (Color online) (a) Structure of $[Cu(NO_3)(pyz)_2]PF_6$ in the a-b plane showing 2D sheets of $[Cu(pyz)_2]^{2+}$ and PF_6^- anions occupying the pores in the structure [12]. The circled region shows sample fluorines near which the muon is expected to localize. (b) Example ZF spectra measured at $T = 5.7$ K with a fit reflecting the configuration shown. *Inset:* proposed F–μ^+ configuration, (top right) the resulting energy levels with allowed transitions and (bottom left) the calculated frequency spectrum.

the spectra reveals that two fluorine spins interact with the μ^+, but not via the linear F–μ^+–F. Instead we find the F–μ^+–F bond angle to be $\theta = 143(1)°$ with F–μ^+ lengths $d_1 = 0.106(3)$ nm and $d_2 = 0.156(3)$ nm. The F–F distance, which is 0.22 nm in the unperturbed material, lengthens to 0.25 nm. This configuration is shown *inset* in Fig. 2. A fit to Eq. 3 resulted in the parameters listed in Table I and is shown in Fig. 2. It should also be expected that other materials containing XF_6^- ions ($X =$Sb or As) will have stopping states of this type.

Case III: Interaction with the HF_2^- ion. The series of coordination polymers $[Cu(HF_2)(pyz)_2]Y$ are formed from infinite 2D sheets of $[Cu(pyz)_2]^{2+}$ in the ab plane (as in the case of $[Cu(NO_3)(pyz)_2]PF_6$ above). These are connected along the c-axis by linear HF_2^- anions to form a pseudo-cubic network. Small tetrahedral or octahedral anions Y occupy the body centred positions in the pseudo-cubic pores [14].

An example spectrum measured above $T_N = 1.94$ K for $[Cu(HF_2)(pyz)_2]ClO_4$ is shown in Fig. 3(b). In this case we would expect the muon to localize near the HF_2^- anion. The spectrum obtained is qualitatively similar to that expected for the interaction of a muon with a single
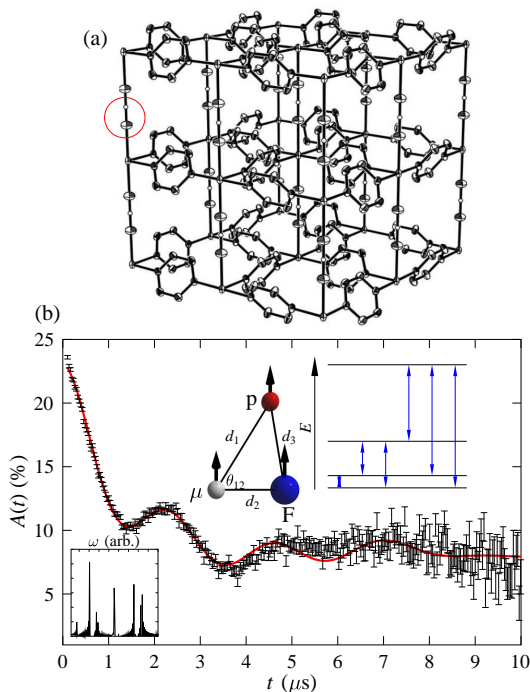
FIG. 3: (Color online) (a) Crystal structure if $[Cu(HF_2)(pyz)_2]X$, with X atoms omitted for clarity. The circled region shows a sample fluorine and proton near which the muon is expected to localize. (b) Example ZF spectra measured at $T = 11$ K with a fit reflecting the configuration shown. *Inset:* proposed F–μ^+–p configuration, (top right) the resulting energy levels with allowed transitions and (bottom left) the calculated frequency spectrum.

an independent molecule in the crystal, the distortion in the other ion positions will be much less significant than the distortion of the two F$^-$ ions. The V_k centre analogy will be less accurate in cases I-III described above, where the non-linear bonds demonstrate that the muon stopping state cannot be regarded as separate from its surroundings. In these cases the tightly bound nature of the fluorine-containing complexes prevents an independent quasi-molecular impurity from forming.

We have presented three examples of the F–μ^+ stopping states in molecular materials. The inherently quantum mechanical interaction of the muon spin leads to entangled states involving the surrounding nuclei and has allowed a characterization of the muon stopping state and facilitates a quantitative estimate of the degree to which the muon distorts its surroundings. These results demonstrate that the introduction of fluorine ions in molecular magnets can provide "traps" for muons, so that the local spin structure in such systems can be probed from well characterized muon sites.

fluorine ion. However, the best fit is obtained if a third spin centre is included. For the tightly bound HF$_2$ ion we might expect this third centre to be that of the nearest proton (see *inset* Fig. 3(b)). This configuration is found to fit the data successfully yielding a F–μ^+ distance of $d_1 = 0.111(3)$ nm, a μ^+–p distance of $d_2 = 0.161(3)$ nm and a F–μ^+–p angle of $\theta = 57(1)°$. The p–F distance d_3, which is 0.11 nm in the unperturbed system, is found to be increased to $d_3 = 0.137(3)$ nm in the presence of the muon. The resulting fit to Eq. (3) results in the fitting parameters given in Table I and is shown in Fig. 3(b).

In addition we note that no dipole-dipole signal is detected from muons stopping near the BF$_4^-$ ion; measurements on Cu(pyz)$_2$(BF$_4$)$_2$ and Cu(C$_5$H$_6$NO)$_6$(BF$_4$)$_2$ [15] do not show a F–μ^+ dipole-dipole signal, while measurements on $[Cu(HF_2)(pyz)_2]BF_4$ [14] show the signal from the HF$_2^-$ ion described above.

In the conventional F–μ^+–F case the F atoms may each shift by large distances (~ 1 Å) from their equilibrium positions towards the μ^+ [5], demonstrating that the muon introduces a non-negligible local distortion in the material. If however, by analogy with the V_k defect center in alkali halides [6], the F–μ^+–F complex acts like

[*] Electronic address: t.lancaster1@physics.ox.ac.uk
[1] S.J. Blundell, Contemp. Phys. **40**, 175 (1999).
[2] R.S. Hayano *et al.*, Phys. Rev. B **20**, 850 (1979).
[3] J.S. Lord, S.P. Cottrell and W.G. Williams, Physica B **289**, 495 (2000).
[4] M. Celio and P.F. Meier, Hyp. Int. **17-19**, 435 (1983).
[5] J.H. Brewer *et al.*, Phys. Rev. B **33**, 7813 (1986).
[6] W. Hayes and A. M. Stoneham, *Defects and Defect Processes in Nonmetallic Solids* (Dover, New York, 2004).
[7] E. Roduner and H. Fischer, Chem. Phys. **54**, 261 (1981).
[8] S. J. Blundell and F. L. Pratt, J. Phys. Condens. Matter **16**, R771 (2004).
[9] T. Lancaster *et al.*, Phys. Rev. B, **73**, 020410(R) (2006).
[10] Zero field (ZF) μ^+SR measurements were made on the MuSR instrument at the ISIS facility. Powder samples were packed in 25 μm Ag foil and mounted on a Ag backing plate inside an Oxford instruments sorption cryostat; http://www.isis.rl.ac.uk/muons/users/equipment/index.htm.
[11] J.L. Manson *et al.*, unpublished.
[12] M.M. Turnbull *et al.*, Mol. Cryst. and Liq. Cryst. **335**, 245 (1999).
[13] F.M. Woodward *et al.* Inorg. Chem. **46** 4256 (2007).
[14] J.L. Manson *et al.* Chem. Comm. 4894 (2006).
[15] T. Lancaster *et al.* unpublished data.